ECTI Transactions on Computer and Information Technology
Journal homepage: https://ph01.tci-thaijo.org/index.php/ecticit/
Published by the ECTI Association, Thailand, ISSN: 2286-9131

Performance Analysis of Downlink NOMA System Relying on Energy Harvesting and Full-Duplex

Chi-Bao Le[1] and Dinh-Thuan Do[2]

ABSTRACT

This paper considers the implementation of wireless power transfer scheme to non-orthogonal multiple access (NOMA) network at downlink. The single antenna power beacon (PB) provide capability of wireless charge to two NOMA users. In addition, full-duplex (FD) scheme is employed for two users. Outage probabilities related to system performance are evaluated in the scenario of the multi-antenna base station. Improved performance can be achieved since multi-antenna, energy harvesting capability. In particular, expressions of outage performance are derived in this system model to help to forward to serve far NOMA users. As the main advantage, NOMA and full-duplex schemes are two advantages and such a system is deployed to enhance the spectral efficiency. Our simulation results will indicate that main parameters such as a power allocation strategy, energy harvesting time, self-interference factor are the main impacts on considered system. The correct derived expressions are presented by matching Monte-Carlo simulation curves and analytical curves in numerical result section. As our main results, FD NOMA system corresponding the first user and the second user exhibits better than OMA 30% and 25% respectively when SNR at the source is 30 dB.

Article information:

Keywords: Full-duplex, Power Beacon, NOMA, Outage Probability, Simultaneous wireless information and power transfer

Article history:
Received: October 11, 2020
Revised: January 8, 2021
Accepted: January 28, 2021
Published: February 12, 2022 (Online)

DOI: 10.37936/ecti-cit.2022161.242809

1. INTRODUCTION

In recent work related to Full-duplex (FD) communication, its advantage motivated many applications since transceivers allow simultaneous downlink (DL) and uplink (UL) transmission over the same frequency band [1–4]. However, FD in this scheme leads to the expense of introducing strong self-interference (SI). A suboptimal precoding and power allocation algorithm is studied to provide maximization of the sum throughput FD systems serving multiple users [2]. In addition, the end-to-end throughput of an FD relay system was evaluated in terms of transmit beamforming design for maximization and the optimal joint receive [3]. The minimum signal-to-interference-plus-noise ratio (SINR) is considered as providing the DL and UL users in a FD system [4]. The authors studied the optimal beamforming and power allocation design [5]. In other improved spectrum efficiency scheme, non-orthogonal multiple access (NOMA) permits multiple users with different transmit power to access the same frequency [6–9]. To separate the different signals, the successive interference cancellation (SIC) is implemented at the receiver [9]. In emerging network of cognitive radio, the NOMA is implemented with cognitive radio networks and it will not only improve the spectrum efficiency but also serve more secondary users. Thanks to advantages of both the cognitive radio and NOMA techniques, and it benefits to the 5th generation mobile networks [10].

The limited performance is resulted from the limited energy supply of small devices in wireless network. In particular, it is hard to replace the battery and/or there is no power line. To overcome this problem, by harvesting the energy from the surrounding environments, they considered energy harvesting technique which is so-called as Radio frequency (RF) energy harvesting [11–15]. In this model, energy harvesting-assisted device is able to harvest the energy from the radio-frequency signals. Such energy

[1]The authors is with Faculty of Electronics Technology, Industrial University of Ho Chi Minh City (IUH), Ho Chi Minh City 700000, Vietnam, E-mail: lechibao@iuh.edu.vn
[2]The authors is with Wireless Communications Research Group, Faculty of Electrical & Electronics Engineering, Ton Duc Thang University, Ho Chi Minh City 700000, Vietnam, E-mail: dodinhthuan@tdtu.edu.vn

harvesting scheme can provide flexible, sustainable and stable energy supply for cognitive radio networks [16–20]. In [17] and [18], the primary spectrum or transmit power in the primary network provide RF energy for the secondary users with dynamically spectrum sensing technique and for battery charging. To enhance the secondary throughput by utilizing the harvested RF energy, an optimal channel selection method is introduced [19]. In cognitive radio sensor networks, the RF energy harvesting was also studied as in [20]. In fact, the RF energy harvesting model is ideal linear in most of recent works related to energy harvesting. However, the non-linear behaviors need be considered in the practical energy harvesting circuits [21–23]. In addition, the non-linear RF energy harvesting model is proposed and examined system performance of the secondary performance [21–23].

In other trends of research, the integration of FD and NOMA was advocated in thanks to the potential benefits of FD transmission [24–26]. In [24], maximization of the weighted system throughput in FD MCNOMA systems can be achieved by studying the optimal power and subcarrier allocation algorithm design. A NOMA-based FD relaying system is evaluated in terms of the outage probability and the ergodic sum rate [25]. In [26], outage probability of NOMA-based FD relaying systems was Investigated by introducing the optimal power allocation minimization.

However, due to little amount of harvested power at users in previous work. Such open problem motivated us to study in this paper a new model of multi-antenna power beacon which serve as wireless charge to far NOMA users.

Table 1: *Key parameters of the system model.*

Symbol	Description
a_i	The power allocation coefficient with $i \in \{1,2\}$, $a_1 + a_2 = 1$ and $a_1 < a_2$
P_S	The transmit power at BS
P_p	The transmit power at PB
n_i	The AWGN noise term followed $\mathbf{n}_{U_i} \sim \mathcal{CN}\left(0, \sigma^2_{U_i}\mathbf{I}_{N_S}\right)$
x_i	The information of U_i
R_i	The target rate at U_i
T	Time duration of signal frame as consideration in Fig. 2
η	The energy conversion efficiency
α	Time percentage to perform wireless power transfer
$\mathbf{h}_1$	The channel link between BS and U_1
$\mathbf{h}_2$	The channel link between BS and U_2
g_1	The channel link between PB and U_1
g_2	The channel link between PB and U_2
f_1	The channel self-interference at U_1
f_2	The channel self-interference at U_2

2. SYSTEM MODEL

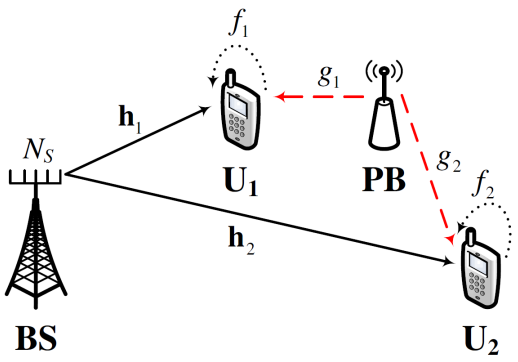

Fig. 1: *System model of wireless powered NOMA system relying power beacon.*

It can be seen from Fig. 1, the system include multi-antenna base station (BS) serves two NOMA users at downlink. It can be facilitated the BS with multiple antennas, N_S. Link BS-user U_1, and link BS-user U_2 are characterized by $\mathbf{h}_1$, $\mathbf{h}_2$, respectively. Two users U_1; U_2 is facilitated with FD mode, f_1; f_2 are self-interference channel related two users U_1; U_2, respectively. In this scenario, wireless charge is served by the power beacon (PB) equipped with one transmit antenna. Then, g_1, g_2 are channels to provide energy harvesting ability to two users.

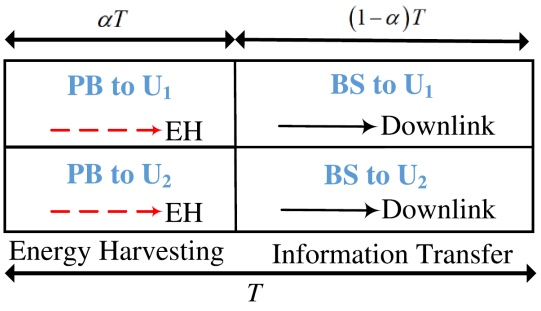

Fig. 2: *Energy harvesting protocol.*

Fig. 2 describes the key parameters related information processing and energy harvesting. In particular, there are two time slots in the time switching-based relaying (TSR) protocol for energy harvesting and information processing at the relay. In Fig. 2, information is transmitted from the source node to the destination node in αT, in which T is the block time, and α is the fraction of the block time allocated for energy harvesting, and its condition is $0 \leq \alpha \leq 1$. The remaining block time, $(1-\alpha)T$ is used information transmission from the source to destination.

It is noted that proper selection of the time fraction, α is important and it is used for optimal amount of harvesting energy at the relay node, and then it affects the achievable throughput at the destination.

The following subsections analyze performance of the energy harvesting and information processing at the relay node.

The channel power gains $\|\mathbf{h}_1\|^2$, $\|\mathbf{h}_2\|^2$, $|g_1|^2$ and $|g_2|^2$ are assumed to be exponentially distributed random variables (RVs) with the parameters Ω_{h_1}, Ω_{h_2}, Ω_{g_1} and Ω_{g_2}, respectively. We call P_S as transmit power of the BS. Especially, the maximum ratio transmission (MRT) is used with beamforming vector to achieve optimal transmission scheme as in [29, 31], with $\|\mathbf{w}_i\| = 1, i = 1, 2$

$$\mathbf{w}_i = \frac{\mathbf{h}_i}{\|\mathbf{h}_i\|} \quad , i \in \{1, 2\}, \tag{1}$$

where $\|.\|$ denotes the Euclidean norm of a matrix. $\mathbf{h}_i \in \mathbb{C}^{N_S \times 1}$ and $g_i \in \mathbb{C}^{1\times 1}$ are the $BS - U_i$ and $PB - U_i$ link channel vector, respectively. During energy harvesting time αT, the harvested energy, E_{U_i} is given by [30, Eq. (2)]

$$E_{U_i} = \begin{cases} \eta P_S \alpha |g_1|^2 T & , i \in 1 \\ \eta P_S \alpha |g_2|^2 T & , i \in 2 \end{cases}, \tag{2}$$

where η is the energy conversion efficiency. Depending on the quality of energy harvesting electric circuitry, $0 < \eta < 1$.

From obtained E_{U_i} in (2), the transmitted power from relay node, P_{U_i} is given by

$$\begin{aligned} P_{U_i} =& E_{U_i}/(1-\alpha)T \\ =& \begin{cases} \eta P_S \alpha |g_1|^2 \Big/ (1-\alpha) & , i \in 1 \\ \eta P_S \alpha |g_2|^2 \Big/ (1-\alpha) & , i \in 2 \end{cases} \end{aligned} \tag{3}$$

To implement NOMA scheme, P_S is also as the normalized transmission powers at the BS. x_1 and x_2 are the signals for U_1 and U_2, respectively while a_1 and a_2 are the corresponding power allocation coefficients. To make better fairness between the relay node, it can be assumed that $a_1 < a_2$, and they are constrained by $a_1 + a_2 = 1$.

During the $k-th$ time slot, U_1 and U_2 receives the superposed signal and loop interference signal simultaneously. The observation at U_1 and U_2 are given by

$$\begin{aligned} \mathbf{y}_{U_1}[k] =& \|\mathbf{h}_1\mathbf{w}_1\| \left(\sqrt{a_1 P_S} x_1[k] + \sqrt{a_2 P_S} x_2[k] \right) \\ &+ \underbrace{\sqrt{P_{U_1}} f_1 x_{LI-1}[k-\tau]}_{self-interference} + \underbrace{\mathbf{n}_{U_1}[k]}_{AWGN} \end{aligned} , \tag{4a}$$

$$\begin{aligned} \mathbf{y}_{U_2}[k] =& \|\mathbf{h}_2\mathbf{w}_2\| \left(\sqrt{a_1 P_S} x_1[k] + \sqrt{a_2 P_S} x_2[k] \right) \\ &+ \underbrace{\sqrt{P_{U_2}} f_2 x_{LI-2}[k-\tau]}_{self-interference} + \underbrace{\mathbf{n}_{U_2}[k]}_{AWGN} \end{aligned} , \tag{4b}$$

where $x_{LI-i}[k-\tau]$ is called as loop interference signal, τ stands for the processing delay at U_i ($i \in \{1, 2\}$) with $\tau \geq 1$ is integer. It is noted that the time k satisfies the relationship $k \geq \tau$. $\mathbf{n}_{U_i}[k]$ the zero mean additive white Gaussian noise (AWGN) vector. These noise terms follow $\mathbf{n}_{U_i} \sim \mathcal{CN}\left(0, \sigma_{U_i}^2 \mathbf{I}_{N_S}\right)$ with equal variance $\sigma_{U_i}^2 \mathbf{I}_N = \sigma^2$ and $f_i \sim \mathcal{CN}(0, \Omega_{f_i})$ is self-interference channel at the U_i.

In NOMA, SIC is required to U_1 first detect U_2 who has a larger transmit power, which has less inference signal. Then the signal of U_2 can be detected from the superposed signal.

Therefore, the received signal-to-interference-plus-noise ratio(SINR) need be computed and such computation performing at U_1 to detect U_2's message x_2

$$\begin{aligned} \gamma_{2\to 1}^{U_1} =& \frac{a_2 P_S \|\mathbf{h}_1\|^2}{a_1 P_S \|\mathbf{h}_1\|^2 + P_{U_1}|f_1|^2 + \sigma^2} \\ =& \frac{a_2 \rho_S \|\mathbf{h}_1\|^2}{a_1 \rho_S \|\mathbf{h}_1\|^2 + \theta |g_1|^2 |f_1|^2 + 1}, \end{aligned} \tag{5}$$

where $\rho_S = \frac{P_S}{\sigma^2}$ is the transmit signal-to-noise radio (SNR) and $\theta = \frac{\eta \rho_S \alpha}{(1-\alpha)}$.

In NOMA, two signals x_1 and x_2 are superimposed at the BS to transmit to far users. They are normalized unity power signals, i.e, $E\{x_1^2\} = E\{x_2^2\} = 1$ in which $E\{.\}$ is the expectation operator.

After SIC, the received SINR at U_1 can be calculated. SINR need be known to detect its own message x_1 and it is given by

$$\gamma_1^{U_1} = \frac{a_1 \rho_S \|\mathbf{h}_1\|^2}{\theta |g_1|^2 |f_1|^2 + 1}. \tag{6}$$

Similarly, the received SINR at U_2 need be computed to detect x_2 and it is formulated by

$$\gamma_2^{U_2} = \frac{a_2 \rho_S \|\mathbf{h}_2\|^2}{a_1 \rho_S \|\mathbf{h}_2\|^2 + \theta |g_2|^2 |f_2|^2 + 1}. \tag{7}$$

3. OUTAGE PROBABILITY ANALYSIS

In preliminary, we assume that all channel coefficients are modeled as independent Rayleigh-distributed random variables (RVs).

It can be denoted that $f_{X_i}(x)$ as the probability density functions (PDFs) of $X_i \triangleq \|\mathbf{h}_i\|^2$ is written as [32]

$$f_{X_i}(x) = \frac{x^{N_S - 1}}{(N_S - 1)! \Omega_{X_i}^{N_S}} e^{-\frac{x}{\Omega_{X_i}}} \quad , i \in \{1, 2\} \tag{8}$$

Next, $F_{X_i}(x)$ is the cumulative distribution function (CDF) of X_i is given by [33]

$$F_{X_i}(x) = 1 - e^{-\frac{x}{\Omega_{X_i}}} \sum_{n=0}^{N_S - 1} \frac{x^n}{n! \Omega_{X_i}^n} \quad , i \in \{1, 2\} \tag{9}$$

Regarding self-interference channel due to FD deployment, $f_{Y_i}(x)$ is the probability density functions

(PDFs) of $Y_i \triangleq |f_i|^2$ is formulated by

$$f_{Y_i}(x) = \frac{1}{\Omega_{Y_i}} e^{-\frac{x}{\Omega_{Y_i}}} \quad , i \in \{1,2\}. \tag{10}$$

We have $F_{Y_i}(x)$ is the cumulative distribution function (CDF) of Y_i is given by

$$F_{Y_i}(x) = 1 - e^{-\frac{x}{\Omega_{Y_i}}} \quad , i \in \{1,2\}. \tag{11}$$

3.1 Analysis on Outage performance in FD mode

In principle, the target rates of relay node are determined since they are related quality of service (QoS). In particular, the outage probability is considered as an important metric and then performance evaluation can be achieved.

We will evaluate the outage performance in two representative users in NOMA in the following.

Outage Probability of U_1:

According to NOMA protocol, the complementary events of outage at U_1 can be required as: U_1 is able to detect x_2 firstly and then it detects its own message x_1. Therefore, the outage probability of U_1 is formulated by

$$\begin{aligned}\mathcal{OP}_{\mathcal{U}_1}^{FD} =& \Pr\left(\gamma_{2\to1}^{U_1} < \gamma_2^{FD} \cup \gamma_1^{U_1} < \gamma_1^{FD}\right)\\ =&1 - \Pr\left(\gamma_{2\to1}^{U_1} \geq \gamma_2^{FD}, \gamma_1^{U_1} \geq \gamma_1^{FD}\right)\\ =&1 - \Pr\left(\|\mathbf{h}_1\|^2 \geq \zeta\left(\theta|g_1|^2|f_1|^2 + 1\right)\right),\end{aligned} \tag{12}$$

where $\gamma_1^{FD} = 2^{R_1} - 1$ with R_1 being the target rate at U_1 to detect x_1 and $\gamma_2^{FD} = 2^{R_2} - 1$ with R_2 being the target rate at U_1 to detect x_2, $\varphi_1 = \frac{\gamma_1^{FD}}{a_1\rho_S}$, $\varphi_2 = \frac{\gamma_2^{FD}}{\rho_S\left(a_2 - \gamma_2^{DL}a_1\right)}$ and $\zeta = \max(\varphi_2, \varphi_1)$

Then, $\mathcal{OP}_{\mathcal{U}_1}^{FD}$ can be solved by

$$\begin{aligned}\mathcal{OP}_{\mathcal{U}_1}^{FD} =&1 - \Pr\left(\|\mathbf{h}_1\|^2 \geq \zeta\left(\theta|g_1|^2|f_1|^2 + 1\right)\right)\\ =&1 - \int_0^\infty f_{|g_1|^2}(x) \int_0^\infty f_{|f_1|^2}(y)\\ &\times \left[1 - F_{\|\mathbf{h}_1\|^2}\left(\zeta\left(\theta xy + 1\right)\right)\right] dxdy\\ =&1 - \sum_{n=0}^{N_S-1} \frac{\zeta^n e^{-\frac{\zeta}{\Omega_{h_1}}}}{n!\Omega_{g_1}\Omega_{f_1}\Omega_{h_1}^n}\\ &\times \int_0^\infty e^{-\frac{x}{\Omega_{g_1}}} \int_0^\infty e^{-y\left(\frac{1}{\Omega_{f_1}} + \frac{\zeta\theta x}{\Omega_{h_1}}\right)}\\ &\times (\theta xy + 1)^n dxdy.\end{aligned} \tag{13}$$

Based on [27, Eq. (1.111)] and [27, Eq. (3.351.3)], $\mathcal{OP}_{\mathcal{U}_1}^{FD}$ is given by

$$\begin{aligned}\mathcal{OP}_{\mathcal{U}_1}^{FD} =&1 - \sum_{n=0}^{N_S-1}\sum_{k=0}^{n} \binom{n}{k} \frac{k!\zeta^n\theta^k\Omega_{f_1}^k}{n!\Omega_{g_1}\Omega_{h_1}^{n-k-1}}\\ &\times e^{-\frac{\zeta}{\Omega_{h_1}}} \int_0^\infty \frac{x^k}{\left(\Omega_{h_1} + \Omega_{f_1}\zeta\theta x\right)^{k+1}} e^{-\frac{x}{\Omega_{g_1}}} dx.\end{aligned} \tag{14}$$

Let $t = \frac{4}{\pi}\arctan(x) - 1 \Rightarrow \tan\left(\frac{\pi(t+1)}{4}\right) = x \Rightarrow \frac{\pi}{4}\sec^2\left(\frac{\pi}{4}(t+1)\right)dt = dx$ with $\sec(x) = \frac{1}{\cos(x)}$, (14) is expressed as

$$\begin{aligned}\mathcal{OP}_{\mathcal{U}_1}^{FD} =&1 - \sum_{n=0}^{N_S-1}\sum_{k=0}^{n} \binom{n}{k} \frac{\pi k!\zeta^n\theta^k\Omega_{f_1}^k}{n!4\Omega_{g_1}\Omega_{h_1}^{n-k-1}}\\ &\times e^{-\frac{\zeta}{\Omega_{h_1}}} \int_{-1}^{1} \sec^2(\pi(t+1)/4)\, e^{-\frac{\tan(\pi(t+1)/4)}{\Omega_{g_1}}}\\ &\times \frac{\tan(\pi(t+1)/4)^k}{\left(\Omega_{h_1} + \Omega_{f_1}\zeta\theta\tan(\pi(t+1)/4)\right)^{k+1}} dt.\end{aligned} \tag{15}$$

Unfortunately, it is difficult to derive a closed-form expression for (15), an accurate approximation can be obtained using Gaussian-Chebyshev quadrature [28, Eq. (25.4.38)], it is given as

$$\begin{aligned}\mathcal{OP}_{\mathcal{U}_1}^{FD} \approx&1 - \sum_{n=0}^{N_S-1}\sum_{k=0}^{n}\sum_{r=1}^{R} \binom{n}{k} \frac{k!\pi^2\zeta^n\theta^k\Omega_{f_1}^k}{n!4R\Omega_{g_1}\Omega_{h_1}^{n-k-1}}\\ &\times \frac{\sqrt{1-\xi_r^2}\sec^2(\pi(\xi_r+1)/4)}{\left(\Omega_{h_1} + \Omega_{f_1}\zeta\theta\tan(\pi(\xi_r+1)/4)\right)^{k+1}}\\ &\times \tan(\pi(\xi_r+1)/4)^k e^{-\frac{\zeta}{\Omega_{h_1}} - \frac{\tan(\pi(\xi_r+1)/4)}{\Omega_{g_1}}},\end{aligned} \tag{16}$$

where $\xi_r = \cos\left(\frac{(2r-1)}{2R}\pi\right)$

Outage Probability of U_2:

The outage probability of U_2 is computed as

$$\begin{aligned}\mathcal{OP}_{\mathcal{U}_2}^{FD} =& \Pr\left(\gamma_2^{U_2} < \gamma_2^{FD}\right)\\ =&1 - \Pr\left(\|\mathbf{h}_2\|^2 < \varphi_2\left(\theta|g_2|^2|f_2|^2 + 1\right)\right)\\ =&1 - \int_0^\infty f_{|g_2|^2}(x) \int_0^\infty f_{|f_2|^2}(y)\\ &\times \bar{F}_{\|\mathbf{h}_2\|^2}(g(x,y))\, dxdy,\end{aligned} \tag{17}$$

where $\bar{F}_{\|\mathbf{h}_2\|^2}(g(x,y)) = \left[1 - F_{\|\mathbf{h}_2\|^2}(\varphi_2(\theta xy + 1))\right]$

Similarly with solving $\mathcal{OP}_{\mathcal{U}_1}^{FD}$, it can be obtained

$\mathcal{OP}_{\mathcal{U}_2}^{FD}$ as

$$\mathcal{OP}_{\mathcal{U}_2}^{FD} \approx 1 - \sum_{n=0}^{N_S-1}\sum_{k=0}^{n}\sum_{q=1}^{Q}\binom{n}{k}\frac{k!\pi^2\varphi_2^n\theta^k\Omega_{f_2}^k}{n!4Q\Omega_{g_2}\Omega_{h_2}^{n-k-1}} \times \frac{\sqrt{1-\xi_q^2}\sec^2\left(\pi\left(\xi_q+1\right)/4\right)}{\left(\Omega_{h_2}+\Omega_{f_2}\varphi_2\theta\tan\left(\pi\left(\xi_q+1\right)/4\right)\right)^{k+1}} \times \tan\left(\pi\left(\xi_q+1\right)/4\right)^k e^{-\frac{\varphi_2}{\Omega_{h_2}}-\frac{\tan\left(\pi\left(\xi_q+1\right)/4\right)}{\Omega_{g_2}}}, \tag{18}$$

where $\xi_q = \cos\left(\frac{(2q-1)}{2Q}\pi\right)$

3.2 Consideration on half-duplex (HD) mode

With HD mode, the received signal at U_i, $i = 1, 2$ node in the downlink of NOMA is given by

$$\mathbf{y}_{U_1}[k] = \|\mathbf{h}_1\mathbf{w}_1\|\left(\sqrt{a_1P_S}x_1[k] + \sqrt{a_2P_S}x_2[k]\right) + \mathbf{n}_{U_1}[k], \tag{19a}$$

$$\mathbf{y}_{U_2}[k] = \|\mathbf{h}_2\mathbf{w}_2\|\left(\sqrt{a_1P_S}x_1[k] + \sqrt{a_2P_S}x_2[k]\right) + \mathbf{n}_{U_2}[k]. \tag{19b}$$

Based on (19a), the outage probabilities with imperfect SIC for the U_1 link they can be written as

$$\begin{aligned}&\mathcal{OP}_{\mathcal{U}_1}^{HD,ipSIC}\\ &= 1 - \Pr\left(\gamma_{2\to1} \geq \gamma_2^{HD}, \gamma_1^{ipSIC} \geq \gamma_1^{HD}\right)\\ &= 1 - \Pr\left(\|\mathbf{h}_1\|^2 \geq \Phi_{\max}, |h_I| \leq \tfrac{1}{\rho_S}\left(\tfrac{\|\mathbf{h}_1\|^2}{\Phi_1} - 1\right)\right),\end{aligned} \tag{20}$$

where $\gamma_{2\to1} = \frac{a_2\rho_S\|\mathbf{h}_1\|^2}{a_1\rho_S\|\mathbf{h}_1\|^2+1}$, $\gamma_1^{ipSIC} = \frac{a_1\rho_S\|\mathbf{h}_1\|^2}{\rho_S|h_I|+1}$, $h_I \sim \mathcal{CN}(0, \Omega_{h_I})$ with Ω_{h_I} $(0 \leq \Omega_{h_I} < 1)$ denotes as the level of residual interference caused by imperfect SIC. More precisely, the value of $\Omega_{h_I} = 0$ and $\Omega_{h_I} < 1$ are the perfect SIC (pSIC) and imperfect SIC (ipSIC), respectively, $\gamma_1^{HD} = 2^{2R_1} - 1$, $\gamma_2^{HD} = 2^{2R_2} - 1$, $\Phi_1 = \frac{\gamma_1^{HD}}{a_1\rho_S}$, $\Phi_2 = \frac{\gamma_2^{HD}}{\rho_S\left(a_2-\gamma_2^{HD}a_1\right)}$ and $\Phi_{\max} = \max(\Phi_1, \Phi_2)$.

By exploiting result from (8), (10) and with the help of the [27, Eq. (3.351.2)], $\mathcal{OP}_{\mathcal{U}_1}^{HD,ipSIC}$ is calculated as

$$\begin{aligned}&\mathcal{OP}_{\mathcal{U}_1}^{HD,ipSIC}\\ &= 1 - \Pr\left(\|\mathbf{h}_1\|^2 \geq \Phi_{\max}, |h_I| \leq \tfrac{1}{\rho_S}\left(\tfrac{\|\mathbf{h}_1\|^2}{\Phi_1} - 1\right)\right)\\ &= 1 - \int_{\Phi_{\max}}^{\infty} f_{\|\mathbf{h}_1\|^2}(x) \int_0^{\frac{1}{\rho_S}\left(\frac{x}{\Phi_1}-1\right)} f_{|h_I|}(y)dxdy\\ &= 1 - \frac{1}{\Gamma(N_S)\Omega_{h_1}^{N_S}}\int_{\Phi_{\max}}^{\infty} x^{N_S-1}e^{-\frac{x}{\Omega_{h_1}}}\\ &\times\left[1 - e^{-\frac{1}{\rho_S\Omega_{h_I}}\left(\frac{x}{\Phi_1}-1\right)}\right]dx\\ &= 1 - \left[e^{-\frac{\Phi_{\max}}{\Omega_{h_1}}}\sum_{r_1=0}^{N_S-1}\frac{\Phi_{\max}^{r_1}}{r_1!\Omega_{h_1}^{r_1}} - \frac{e^{\chi}}{\Omega_{h_1}^{N_S}\Xi^{N_S}}\sum_{r_2=0}^{N_S-1}\frac{\Phi_{\max}^{r_1}\Xi^{r_2}}{r_2!}\right],\end{aligned} \tag{21}$$

where $\Xi = \frac{1}{\Omega_{h_1}} + \frac{1}{\rho_S\Phi_1\Omega_{h_I}}$, $\chi = \frac{1}{\rho_S\Omega_{h_I}} - \frac{\Phi_{\max}}{\Xi}$ and $\Gamma(x) = (x-1)!$ is the Gamma function

Based on (19b), the outage probabilities with perfect SIC for the U_2 link they can be written as

$$\begin{aligned}\mathcal{OP}_{\mathcal{U}_2}^{HD} &= 1 - \Pr\left(\gamma_2 \geq \gamma_1^{HD}\right)\\ &= F_{\|\mathbf{h}_2\|^2}\left(\frac{\gamma_1^{HD}}{\rho_S\left(a_2 - a_1\gamma_1^{HD}\right)}\right)\\ &= 1 - e^{-\frac{\gamma_1^{HD}}{\Omega_{h_1}\rho_S\left(a_2-a_1\gamma_1^{HD}\right)}}\\ &\times\sum_{n=0}^{N_S-1}\frac{\left(\gamma_1^{HD}\right)^n}{n!\rho_S^n\left(a_2 - a_1\gamma_1^{HD}\right)^n\Omega_{h_2}^n},\end{aligned} \tag{22}$$

where $\gamma_2 = \frac{a_2\rho_S\|\mathbf{h}_2\|^2}{a_1\rho_S\|\mathbf{h}_2\|^2+1}$

3.3 Asymptotic Outage Probability Analysis for Two User's

We conduct the asymptotic outage probability analysis in the high SNR region. Based on analytical result in (16) and (18), when $\rho_S \to \infty$, the asymptotic outage probability of U_1 and U_2 for FD NOMA with $e^{-x} \to 1 - x$ is given by

$$\mathcal{OP}_{\mathcal{U}_1}^{FD,\infty} \approx 1 - \sum_{n=0}^{N_S-1}\sum_{k=0}^{n}\sum_{r=1}^{R}\binom{n}{k}\frac{k!\pi^2\zeta^n\theta^k\Omega_{f_1}^k}{n!4R\Omega_{g_1}} \times \Omega_{h_1}^{k+1-n}\Upsilon(\xi_r)\tan\left(\pi\left(\xi_r+1\right)/4\right)^k \times\left(1 - \frac{\zeta}{\Omega_{h_1}}\right)e^{-\frac{\tan\left(\pi\left(\xi_r+1\right)/4\right)}{\Omega_{g_1}}}, \tag{23}$$

and

$$\mathcal{OP}_{\mathcal{U}_2}^{FD,\infty} \approx 1 - \sum_{n=0}^{N_S-1}\sum_{k=0}^{n}\sum_{q=1}^{Q}\binom{n}{k}\frac{k!\pi^2\varphi_2^n\theta^k\Omega_{f_2}^k}{n!4Q\Omega_{g_2}} \times \Omega_{h_2}^{k+1-n}\Psi(\xi_q)\tan\left(\pi\left(\xi_q+1\right)/4\right)^k \times\left(1 - \frac{\varphi_2}{\Omega_{h_2}}\right)e^{-\frac{\tan\left(\pi\left(\xi_q+1\right)/4\right)}{\Omega_{g_2}}}, \tag{24}$$

where $\xi_r = \cos\left(\frac{(2r-1)}{2R}\pi\right)$, $\xi_q = \cos\left(\frac{(2q-1)}{2Q}\pi\right)$, $\Upsilon(x) = \frac{\sqrt{1-x^2}\sec^2(\pi(x+1)/4)}{\left(\Omega_{h_1}+\Omega_{f_1}\zeta\theta\tan(\pi(x+1)/4)\right)^{k+1}}$ and $\Psi(x) = \frac{\sqrt{1-x^2}\sec^2(\pi(x+1)/4)}{4Q\left(\Omega_{h_2}+\Omega_{f_2}\varphi_2\theta\tan(\pi(x+1)/4)\right)^{k+1}}$.

The same situation can be seen for HD mode, the asymptotic outage probability of U_1 and U_2 for HD NOMA with $e^{-x} \to 1-x$ is given by

$$\mathcal{OP}_{\mathcal{U}_1}^{HD,ipSIC,\infty} = 1 - \left[\left(1-\frac{\Phi_{\max}}{\Omega_{h_1}}\right)\sum_{r_1=0}^{N_S-1}\frac{\Phi_{\max}^{r_1}}{r_1!\Omega_{h_1}^{r_1}} - \frac{(1-\chi)}{\Omega_{h_1}^{N_S}\Xi^{N_S}}\sum_{r_2=0}^{N_S-1}\frac{\Phi_{\max}^{r_1}\Xi^{r_2}}{r_2!}\right], \tag{25}$$

and

$$\mathcal{OP}_{\mathcal{U}_2}^{HD,\infty} = 1 - \left(1-\frac{\gamma_1^{HD}}{\rho_S\left(a_2-a_1\gamma_1^{HD}\right)}\right) \times \sum_{n=0}^{N_S-1}\frac{\left(\gamma_1^{HD}\right)^n}{n!\rho_S^n\left(a_2-a_1\gamma_1^{HD}\right)^n\Omega_{h_1}^n}. \tag{26}$$

4. NUMERICAL RESULTS

To confirm accuracy of the proposed analytical expressions in term of the outage probabilities, this section provides the simulated results which are derived in the previous section. Furthermore, the lowest outage performance can be analyzed to evaluate the performances of such NOMA system under different simulated parameters. Finally, the effect of main parameters on the performances is further determined. We use $a_1 = 0.2$ and $a_2 = 0.8$ as power allocation factors. Regarding energy harvesting, we set $\eta = 1$ and $\alpha = 0.2$. Target rates are $R_1 = 2$ and $R_2 = 1$. To perform approximate computation, $Q = R = 500$. The channel gains are $\Omega_{h_1} = \Omega_{g_1} = 0.6$, $\Omega_{g_2} = \Omega_{h_2} = 0.5$ and $\Omega_{f_1} = \Omega_{f_2} = 0.01$.

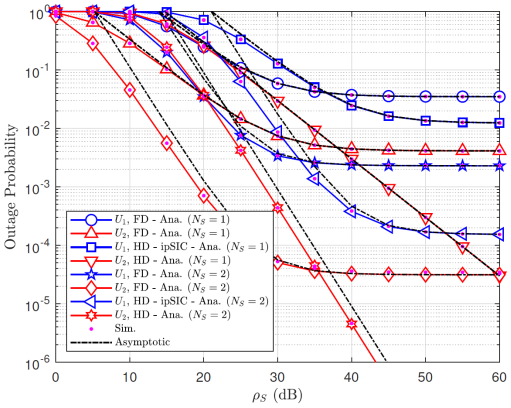

Fig.3: *Outage probability versus ρ_S at U_1 and U_2, with $\Omega_{h_I} = -40$ (dB)*

In Fig. 3, the curves of outage probability for two NOMA users versus transmit SNR ρ_S at the BS is observed. It can be seen clearly that the theoretical curves achieved by mathematical analysis shows a considerable match with the Monte Carlo simulations. The saturation trends can be seen it FD mode for both users at high SNR, as ρ_S is greater than 40 (dB). The reason is that self-interference exists due to FD mode and it make system performance become worse. The figure clearly shows that with increased SNR at the BS, outage will be improved significantly. It is confirmed that outage performance of user U_2 is better than that of user U_1. It can be explained that performance gap exist due to different power allocated a_1; a_2. In contrast with FD mode, higher SNR leads to improved outage at HD mode. Furthermore, asymptotic curves tend to locate near to the curves of exact computation.

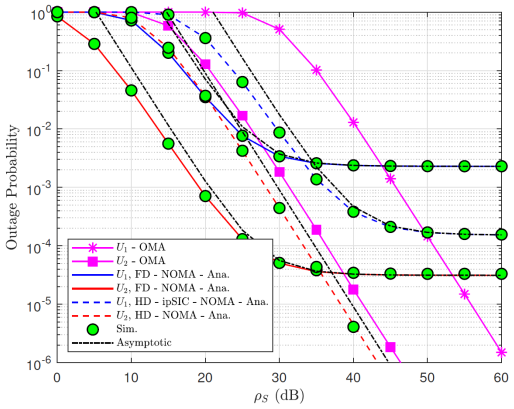

Fig.4: *Comparison on NOMA and OMA, with $\Omega_{h_I} = -40$ (dB).*

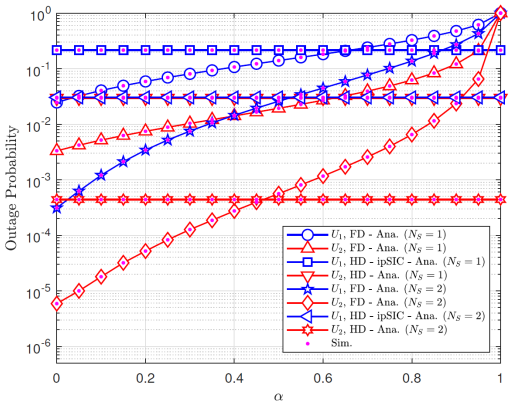

Fig.5: *Outage probability versus time-aware energy harvesting factor α, with $\rho_S = 30$ (dB) and $\Omega_{h_I} = -30$ (dB).*

Next, in Fig. 4, we investigate performance differences between OMA and NOMA. It can be observed that outage behavior in NOMA with HD mode is still

better than that if OMA in entire SNR region.

Regarding energy harvesting, Fig. 5 evaluate impact of level of harvested energy α on the outage probability in FD mode. The reason is that in FD mode, self-interference channel is resulted from harvested power. Increasing percentage of harvested power leads to worse performance because less time for information processing. While HD mode does not depend on interference channel, and then outage performance keeps stable in whole range of α.

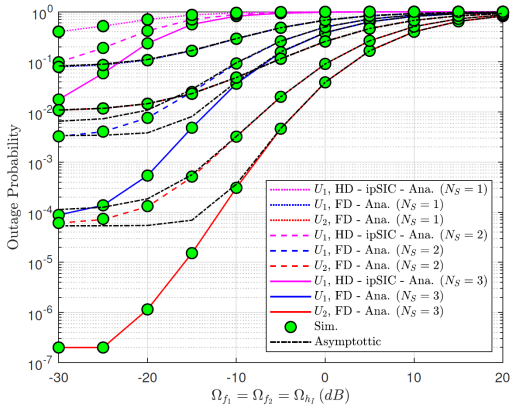

Fig. 6: *Impact of self-interference channel on outage behavior, with* $\rho_S = 25$ *(dB).*

Regarding energy harvesting, Fig. 6 evaluate impact of level of interference on the outage probability in FD mode. Furthermore, as in previous figures, more antennas equipped at the BS lead to better outage performance.

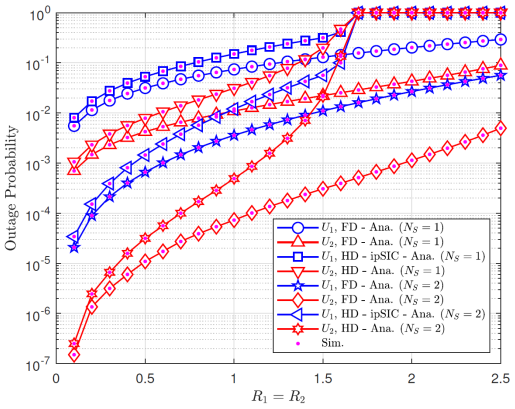

Fig. 7: *Outage performance versus fixed data rates* R_1 *and* R_2*, with* $\rho_S = 25$ *(dB),* $\Omega_{h_I} = -40$ *(dB),* $a_1 = 0.1$ *and* $a_2 = 0.9$*.*

Fig. 7 plots the outage probability for two NOMA users as increasing target rates. The performance gap among two users remains at low region from 0.5 to 1.5, but at high required data rate, system meets outage event.

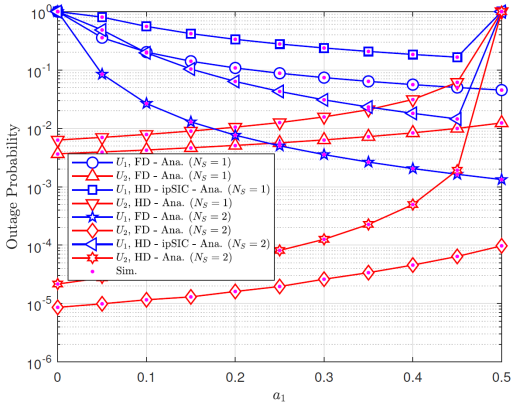

Fig. 8: *Outage probabilities versus* a_1*, with* $\Omega_{h_I} = -40$ *(dB),* $R_1 = 2$*,* $R_2 = 0.5$ *and* $\rho_S = 25$ *(dB).*

Fig. 8 shows the impact of power allocation coefficient a_1 on the outage event of considered schemes. It is confirmed that outage performance of U_2 better than that of U_1 at very low value of a_1. Interestingly, optimal outage for user U_1 in HD mode can be achieved at $a_1 = 0.5$.

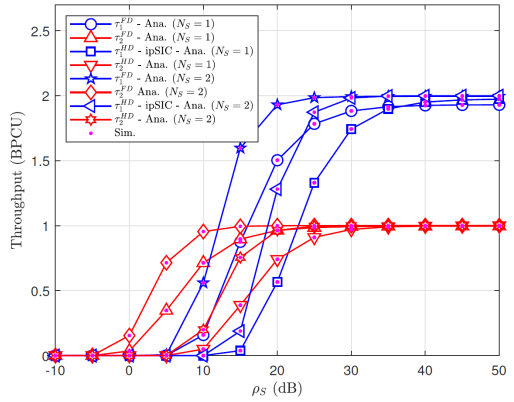

Fig. 9: *Throughput performance of two relays node, with* $\Omega_{h_I} = -40$ *(dB),* $R_1 = 2$ *and* $R_2 = 1$*.*

As seen from Fig. 9, since the throughput is computed based on achievable outage probability, it can be further evaluate throughput in delay-limited transmission mode as $\tau_\ell^\iota = (1 - \mathcal{OP}_\ell^\iota) R_\ell$ with $\ell \in \{1, 2\}$ and $\iota \in \{FD, HD\}$. The throughput of two relays node increase significantly since data rates are main factor. It is seen clearly that throughput increases once data rates increase.

5. CONCLUSION

In this paper, we developed a theoretical framework to analyze NOMA downlink system performance under deployment of FD mode and energy harvesting. Analytical results are derived to show reasonable outage performance. For the downlink NOMA system, two different outage performance of

two users can be shown due to different power allocation factors for each NOMA user. The study shows that increasing transmit SNR leads to significant performance improvement. It is also provided guidelines as reasonable selection of the number of antennas at the BS are performed, outage probability meets ideal value.

ACKNOWLEDGMENT

The authors would like to thank the anonymous reviews for the helpful comments and suggestions. This research is supported by Industrial University of Ho Chi Minh City (IUH) under grant number 60/HD-DHCN.

References

[1] D. Bharadia, E. McMilin and S. Katti, "Full Duplex Radios," in *Proc. ACM SIGCOMM Conf.*, pp. 375–386, 2013.

[2] D. Nguyen, L.-N. Tran, P. Pirinen and M. Latva-aho, "On the Spectral Efficiency of Full-Duplex Small Cell Wireless Systems," *IEEE Trans. Wireless Commun.*, vol. 13, no. 9, pp. 4896-4910, 2014.

[3] M. Mohammadi, B. K. Chalise, H. A. Suraweera, C. Zhong, G. Zheng and I. Krikidis, "Throughput Analysis and Optimization of WirelessPowered Multiple Antenna Full-Duplex Relay Systems," *IEEE Trans. Commun.*, vol. 64, no. 4, pp. 1769-1785, 2016.

[4] T.-H. Chang, Y.-F. Liu and S.-C. Lin, "Max-Min-Fairness Linear Transceiver Design for Full-Duplex Multiuser Systems," in *Proc. IEEE Intern. Workshop on Signal Process. Advances in Wireless Commun.*, pp. 1-5, 2017.

[5] X.-X. Nguyen and Dinh-Thuan Do, "Optimal power allocation and throughput performance of full-duplex DF relaying networks with wireless power transfer-aware channel," *EURASIP Journal on Wireless Communications and Networking*, vol. 2017, no. 1, pp. 152, 2017.

[6] X.-X. Nguyen and Dinh-Thuan Do, "Maximum Harvested Energy Policy in Full-Duplex Relaying Networks with SWIPT," *International Journal of Communication Systems (Wiley)*, vol 30, no. 17, 2017.

[7] Z. Ding et al., "Application of non-orthogonal multiple access in LTE and 5G networks," *IEEE Commun. Mag.*, vol. 55, no. 2, pp. 185-191, 2017.

[8] Z. Ding, X. Lei, G. K. Karagiannidis, R. Schober, J. Yuan and V. K. Bhargava. "A survey on non-orthogonal multiple access for 5G networks: Research challenges and future trends," *IEEE J. Sel. Areas Commun.*, vol. 35, no. 10, pp. 2181-2195, 2017.

[9] F. Fang, H. Zhang, J. Cheng, S. Roy and V. C. M. Leung, "Joint user scheduling and power allocation optimization for energy-efficient NOMA systems with imperfect CSI," *IEEE J. Sel. Areas Commun.*, vol. 35, no. 12, pp. 2874-2885, 2017.

[10] F. Zhou, Y. Wu, Y.-C. Liang, Z. Li, Y. Wang and K.-K. Wong, "State of the art, taxonomy, and open issues on cognitive radio networks with NOMA," *IEEE Wireless Commun.*, vol. 25, no. 2, pp. 100-108, Apr. 2018.

[11] K. Woradit, S. Srirai, S. Kitjarunerungroj, T. Kodmatcha and P. Sangmahamad, "Multi-user Secrecy SWIPT for 5G OFDMA Networks with Particle Swarm Optimizations," 2019 IEEE International Conference on Consumer Electronics - Asia (ICCE-Asia), Bangkok, Thailand, 2019, pp. 1-5, doi: 10.1109/ICCE-Asia46551.2019.8941603.

[12] D.-T. Do, "Optimal Throughput under Time Power Switching based Relaying Protocol in Energy Harvesting Cooperative Network," *Wireless Personal Communications (Springer)*, vol. 87, no. 2, pp. 551-564, 2016.

[13] D.-T. Do, "Power Switching Protocol for Two-way Relaying Network under Hardware Impairments," *Radioengineering*, vol. 24, no. 3, pp. 765-771, 2015.

[14] D.-T. Do, H.-S. Nguyen, M. Voznak and T.-S. Nguyen, "Wireless powered relaying networks under imperfect channel state information: system performance and optimal policy for instantaneous rate," *Radioengineering*, vol. 26, no. 3, pp. 869-877, 2017.

[15] H.-S. Nguyen, D.-T. Do, T.-S. Nguyen and M. Voznak, "Exploiting hybrid time switching-based and power splitting-based relaying protocol in wireless powered communication networks with outdated channel state information," *Automatika*, vol. 58, no. 4, pp. 111-118, 2017.

[16] D.-T. Do, "Energy-aware two-way relaying networks under imperfect hardware: optimal throughput design and analysis," *Telecommunication Systems*, vol. 62, no. 2, pp. 449-459, 2016.

[17] H. Hu, Y.-C. Liang, H. Zhang and B.-H. Soong. "Cognitive radio with self-power recycling," *IEEE Trans. Veh. Technol.*, vol. 66, no. 7, pp. 6201-6214, 2017.

[18] A. Celik, A. Alsharoa and A. E. Kamal, "Hybrid energy harvesting-based cooperative spectrum sensing and access in heterogeneous cognitive radio networks," *IEEE Trans. Cogn. Commun. Netw.*, vol. 3, no. 1, pp. 37-48, 2017.

[19] M. Pratibha, K. H. Li and K. C. Teh, "Channel selection in multichannel cognitive radio systems employing RF energy harvesting," *IEEE Trans. Veh. Technol.*, vol. 65, no. 1, pp. 457-462, 2016.

[20] J. Ren, J. Hu, D. Zhang, H. Guo, Y. Zhang and X. Shen, "RF energy harvesting and transfer in cognitive radio sensor networks: Opportunities and challenges," *IEEE Commun. Mag.*, vol. 56, no. 1, pp. 104-110, 2018.

[21] J.-M. Kang, I.-M. Kim and D. I. Kim, "Wireless information and power transfer: Rate-energy tradeoff for nonlinear energy harvesting," *IEEE Trans. Wireless Commun.*, vol. 17, no. 3, pp. 1966-1981, 2018.

[22] S. Wang, M. Xia, K. Huang and Y.-C. Wu, "Wirelessly powered two-way communication with nonlinear energy harvesting model: Rate regions under fixed and mobile relay," *IEEE Trans. Wireless Commun.*, vol. 16, no. 12, pp. 8190-8204, 2017.

[23] R. Morsi, D. S. Michalopoulos and R. Schober, "Performance analysis of near-optimal energy buffer aided wireless powered communication," *IEEE Trans. Wireless Commun.*, vol. 17, no. 2, pp. 863-881, 2018.

[24] Y. Sun, D. W. K. Ng, Z. Ding and R. Schober, "Optimal Joint Power and Subcarrier Allocation for Full-Duplex Multicarrier Non-Orthogonal Multiple Access Systems," *IEEE Trans. Commun.*, vol. 65, no. 3, pp. 1077-1091, 2017.

[25] C. Zhong and Z. Zhang, "Non-Orthogonal Multiple Access with Cooperative Full-Duplex Relaying," *IEEE Commun. Lett.*, vol. 20, no. 12, pp. 2478-2481, Dec 2016.

[26] L. Zhang, J. Liu, M. Xiao, G. Wu, Y. C. Liang and S. Li, "Performance Analysis and Optimization in Downlink NOMA Systems with Cooperative Full-Duplex Relaying," *IEEE J. Select. Areas Commun.*, vol. 35, no. 10, pp. 2398-2412, 2017.

[27] I. S. Gradshteyn and I. M. Ryzhik. *Table of Integrals, Series and Products*, 6th ed. New York, NY, USA: Academic Press, 2000.

[28] M. Abramowitz and I. A. Stegun, *Handbook of Mathematical Functions with Formulas, Graphs, and Mathematical Tables*. New York, NY, USA: Dover, 1972.

[29] W. Huang, H. Chen, Y. Li, and B. Vucetic, "On the performance of multi-antenna wireless-powered communications with energy beamforming," *IEEE Trans. on Vehicular Technology*, vol. 65, pp. 1801-1808, 2016.

[30] A. A. Nasir, X. Zhou, S. Durrani, and R. A. Kennedy, "Relaying protocols for wireless energy harvesting and information processing," *IEEE Trans. Wireless Commun.*, vol. 12, no. 7, pp. 3622-3636, 2013.

[31] Nguyen, X.X.; Do, D.T, "An Adaptive-Harvest-Then-Transmit Protocol for Wireless Powered Communications: Multiple Antennas System and Performance Analysis," *KSII Transaction Internet Inf. Syst.*, vol. 11, no. 4, pp. 1889-1910, 2017.

[32] K. Woradit, T. Q. S. Quek and Z. Z. Lei, "Cooperative multicell ARQ in MIMO cellular systems," 2010 *IEEE 11th International Workshop on Signal Processing Advances in Wireless Communications (SPAWC)*, Marrakech, 2010, pp. 1-5, doi: 10.1109/SPAWC.2010.5670997.

[33] K. Woradit, T. Q. S. Quek and Z. Lei, "Cooperative Multicell ARQ - Packet Error Rate and Throughput Analysis," 2010 *IEEE Wireless Communication and Networking Conference*, Sydney, NSW, 2010, pp. 1-6, doi: 10.1109/WCNC.2010.5506698.

Chi-Bao Le was born in Binh Thuan province, Vietnam. He has worked closely with Dr. Thuan at Wireless Communications and Signal Processing Research Group at Industrial University of Ho Chi Minh City, Vietnam. He is currently pursued Master degree in the field of wireless communications. His research interest includes electronic design, signal processing in wireless communications network, non-orthogonal multiple access, physical layer security and reconfigurable intelligent surfaces.

Dinh-Thuan Do received the B.S. degree, M.Eng. degree, and Ph.D. degree from Vietnam National University (VNU-HCMC) in 2003, 2007, and 2013 respectively, all in Communications Engineering. He was a visiting Ph.D. student with Communications Engineering Institute, NationalTsing Hua University, Taiwan from 2009 to 2010. Prior to joining Ton Duc Thang University, he was senior engineer at the VinaPhone Mobile Network from 2003 to 2009. Dr. Thuan was recipient of golden Globe Award from Vietnam Ministry of Science and Technology in 2015 (Top 10 most excellent scientist nationwide). His name and his achievements will be reported in a special book entitled "Young talents in Vietnam 2015-2020". His research interest includes signal processing in wireless communications networks, NOMA, full-duplex transmission, and energy harvesting. His publications include over 80 SCIE/SCI-indexed journal papers, over 45 SCOPUS-indexed journal papers and over 50 international conference papers. He is sole author in 1 textbook and 1 book chapter. Heis currently serving as Editor of Computer Communications (Elsevier), Associate Editor of EURASIP Journal on Wireless Communications and Networking (Springer), and Editor of KSII Transactions on Internet and Information Systems.